Cecília Fonseca; Luísa Pereira; Helena Ferreira; Ana Paula Martins

Generalized madogram and pairwise dependence of maxima over two regions of a random field

Kybernetika, Vol. 51 (2015), No. 2, 193–211

Persistent URL: http://dml.cz/dmlcz/144291

KYBERNETIKA — VOLUME *51* (2015), NUMBER 2, PAGES 193–211

GENERALIZED MADOGRAM AND PAIRWISE DEPENDENCE OF MAXIMA OVER TWO REGIONS OF A RANDOM FIELD

C. Fonseca, L. Pereira, H. Ferreira and A. P. Martins

Spatial environmental processes often exhibit dependence in their large values. In order to model such processes their dependence properties must be characterized and quantified. In this paper we introduce a measure that evaluates the dependence among extreme observations located in two disjoint sets of locations of $\mathbb{R}^2$. We compute the range of this new dependence measure, which extends the existing λ-madogram concept, and compare it with extremal coefficients, finding generalizations of the known relations in the pairwise approach. Estimators for this measure are introduced and asymptotic normality and strong consistency are shown. An application to the annual maxima precipitation in Portuguese regions is presented.

Keywords: max-stable random field, dependence coefficients, extreme values

Classification: 60G70

1. INTRODUCTION

Natural models for spatial extremes, as observed in environmental, atmospheric and geological sciences, are max-stable processes. These processes arise from an infinite-dimensional generalization of extreme value theory and date back to de Haan [4], Vatan [19] and de Haan and Pickands [5], who obtained, among other results, a spectral representation of such processes. Max-stable processes can be, for example, good approximations for annual maxima of daily spatial rainfall (Smith [16], Coles [3], Schlather [14], among others) and therefore have been widely applied to real data.

Briefly, a max-stable process $\mathbf{Z} = \{Z_{\boldsymbol{x}}\}_{\boldsymbol{x}\in\mathbb{R}^d}$ is the limit process of maxima of independent and identically distributed (i.i.d.) random fields $Y_{\boldsymbol{x}}^{(i)}$, $\boldsymbol{x} \in \mathbb{R}^d$, $i = 1, \ldots, n$. Namely, for suitable $a_n(\boldsymbol{x}) > 0$ and $b_n(\boldsymbol{x}) \in \mathbb{R}$,

$$Z_{\boldsymbol{x}} = \lim_{n\to\infty} \frac{\bigvee_{i=1}^n Y_{\boldsymbol{x}}^{(i)} - b_n(\boldsymbol{x})}{a_n(\boldsymbol{x})}, \qquad \boldsymbol{x} \in \mathbb{R}^d,$$

provided the limit exists, where $\bigvee_{i=1}^n Y_{\boldsymbol{x}}^{(i)} = \max\{Y_{\boldsymbol{x}}^{(1)}, \ldots, Y_{\boldsymbol{x}}^{(n)}\}$.

The distribution of $(Z_{\boldsymbol{x}_1}, \ldots, Z_{\boldsymbol{x}_k})$ is a multivariate extreme value (MEV) distribution G where its margins are univariate extreme value distribution functions themselves.

DOI: 10.14736/kyb-2015-2-0193

We can assume, without loss of generality, that the margins of $\mathbf{Z}$ have a unit Fréchet distribution, $F(x) = \exp(-x^{-1})$, $x > 0$ (Resnick [12]). This assumption on the margins is particularly useful since the max-stable distribution G can then be written as

$$G(\mathbf{z}) = \exp(-V(\mathbf{z})), \quad \text{with } \mathbf{z} = (z_1, \ldots, z_k) \text{ and } z_i \in \mathbb{R}^+,$$

where V denotes the dependence function of the MEV distribution G, which is homogeneous of order -1, i. e., $V(\alpha\, \mathbf{z}) = \alpha^{-1} V(\mathbf{z})$, $\mathbf{z} = (z_1, \ldots, z_k)$, $z_i \in \mathbb{R}^+$, $\alpha > 0$. Observe that $V(\mathbf{z}) = \infty$ as soon as $z_j = 0$ for some $j = 1, \ldots, k$. Also, since the margins of G are unit Fréchet $V(\infty, \ldots, \infty, z_j, \infty, \ldots, \infty) = z_j^{-1}$ for all $j = 1, \ldots, k$ and $0 < z_j < \infty$.

The dependence function captures the multivariate dependence structure and the scalar $V(\mathbf{1})$, $\mathbf{1} = (1, \ldots, 1)$ defines the extremal coefficient considered in Schlather and Tawn [15] which measures the extremal dependence between the variables $Z_{\boldsymbol{x}_1}, \ldots, Z_{\boldsymbol{x}_k}$. This coefficient varies between 1 and k depending on the degree of dependence among the k variables. These measures of dependence have gained great importance since quantifying dependence between extreme events occurring at several locations of a random field is a fundamental issue in applied spatial extreme value analysis.

Cooley et al. [2] showed that the bivariate extremal coefficient can be directly estimated from the madogram (that represents a first order variogram), obtaining in this way a connection between extreme value theory and the field of geostatistics. An estimate of the full pairwise extremal dependence function is given by the λ-madogram defined in Naveau et al. [10] as

$$\nu^{\lambda}(\boldsymbol{x}_1, \boldsymbol{x}_2) = \frac{1}{2} E \left| F^{\lambda}(Z_{\boldsymbol{x}_1}) - F^{1-\lambda}(Z_{\boldsymbol{x}_2}) \right|, \quad \lambda \in (0, 1), \tag{1}$$

where F denotes the marginal distribution of $\mathbf{Z}$.

Although the λ-madogram fully characterizes the pairwise extremal dependence it does not enable the analysis of dependence between maxima over two disjoint regions of locations, where by a region of locations of $\mathbb{R}^2$ we mean a set of locations of $\mathbb{R}^2$. The importance of characterizing dependence between extremes occurring at two disjoint regions has been recognized by hydrologists who have grouped data into regions based on geographical or catchment characteristics. It is clear that, for example, the weather in mountain regions usually affects the weather in the surrounding regions and therefore a measure able to capture such regional dependence is essential.

In this paper we propose a measure that enables the analysis of dependence between maxima over two disjoint regions of locations $\mathbf{x} = \{\boldsymbol{x}_1, \ldots, \boldsymbol{x}_k\}$ and $\mathbf{y} = \{\boldsymbol{y}_1, \ldots, \boldsymbol{y}_s\}$ and therefore generalizes the λ-madogram. This measure, here called generalized madogram, is introduced in Section 2 and some of its main properties are presented, namely its relation with the dependence function of the MEV G. In Section 3 we present estimators for the generalized madogram and derive the respective properties of strong consistency and asymptotic normality. The performance of the proposed estimators is analyzed in Section 4 with a max-stable M4 random field. Finally, Section 5 illustrates our approach through an application to precipitation data from Portugal. Section 6 is devoted to conclusions. Proofs are sketched in the Appendix.

2. GENERALIZED MADOGRAM AND DEPENDENCE OF SPATIAL EXTREME EVENTS

In modeling spatial extremes, both the madogram and the pairwise extremal coefficient approach rely on pairs of locations. A natural improvement is considering a measure which moves beyond pairs and considers disjoint sets of locations.

Next, we introduce the generalized madogram which is an extension of Naveau *et al.*'s [10]. We also consider a max-stable random field $Z = \{Z_{\boldsymbol{x}}\}_{\boldsymbol{x}\in\mathbb{R}^2}$ with unit Fréchet margins, but instead of building the pairwise bivariate distribution of this process as provided by the λ-madogram, we consider two regions of locations $\mathbf{x} = \{\boldsymbol{x}_1, \ldots, \boldsymbol{x}_k\}$ and $\mathbf{y} = \{\boldsymbol{y}_1, \ldots, \boldsymbol{y}_s\}$ and we model the dependence of the maxima over $\mathbf{x}$ and $\mathbf{y}$ as follows.

Definition 2.1. Let $Z = \{Z_{\mathbf{x}}\}_{\mathbf{x}\in\mathbb{R}^2}$ be a max-stable random field with unit Fréchet margins and $\boldsymbol{x} = \{\mathbf{x}_1, \ldots, \mathbf{x}_k\}$ and $\boldsymbol{y} = \{\mathbf{y}_1, \ldots, \mathbf{y}_s\}$ two disjoint regions of $\mathbb{R}^2$. The generalized madogram is defined as

$$\nu^{\alpha,\beta}(\mathbf{x},\mathbf{y}) = \frac{1}{2}E\left|F^{\alpha}(M(\mathbf{x})) - F^{\beta}(M(\mathbf{y}))\right|, \quad \alpha > 0,\ \beta > 0, \tag{2}$$

where $M(\boldsymbol{x}) = \bigvee_{i=1}^{k} Z_{\mathbf{x}_i}$ and $M(\boldsymbol{y}) = \bigvee_{j=1}^{s} Z_{\mathbf{y}_j}$.

Remark 2.2. When we take $\beta = 1-\alpha$, $\alpha \in (0,1)$, and $k = s = 1$ in (2), we obtain (1).

Remark 2.3. Since F is a continuous distribution function, the following equalities hold for the generalized madogram

$$\begin{aligned}\nu^{\alpha,\beta}(\mathbf{x},\mathbf{y}) &= \frac{1}{2}E\left|\bigvee_{i=1}^{k} F^{\alpha}(Z_{\boldsymbol{x}_i}) - \bigvee_{j=1}^{s} F^{\beta}(Z_{\boldsymbol{y}_j})\right| \\ &= \frac{1}{2}E\left|\bigvee_{i=1}^{k} F\left(\frac{Z_{\boldsymbol{x}_i}}{\alpha}\right) - \bigvee_{j=1}^{s} F\left(\frac{Z_{\boldsymbol{y}_j}}{\beta}\right)\right|.\end{aligned} \tag{3}$$

This representation of the generalized madogram, $\nu^{\alpha,\beta}(\mathbf{x},\mathbf{y})$, naturally gives rise to the estimators for this coefficient, defined in Section 3.

Remark 2.4. From (3) it is clear that similarly to the λ-madogram the constants α and β are the weights of the locations and a practical choice can be $\alpha + \beta = 1$. A wise choice when there are no privileging locations in each region $\mathbf{x} = \{\boldsymbol{x}_1, \ldots, \boldsymbol{x}_k\}$ and $\mathbf{y} = \{\boldsymbol{y}_1, \ldots, \boldsymbol{y}_s\}$ and that generalizes the bivariate approach, is to consider $\alpha = \frac{\lambda}{k}$ and $\beta = \frac{1-\lambda}{s}$, $\lambda \in (0,1)$.

The following proposition states that $\nu^{\alpha,\beta}(\mathbf{x},\mathbf{y})$ provides dependence information between the regions $\mathbf{x}$ and $\mathbf{y}$ through the dependence function of the MEV distribution G. This result generalizes Proposition 1. in Naveau et al. [10].

Proposition 2.5. For any max-stable random field with unit Fréchet margins and for each pair of disjoint regions of locations $\mathbf{x} = \{\mathbf{x}_1, \ldots, \mathbf{x}_k\}$ and $\mathbf{y} = \{\mathbf{y}_1, \ldots, \mathbf{y}_s\}$ in $\mathbb{R}^2$, we have

$$\nu^{\alpha,\beta}(\mathbf{x},\mathbf{y}) = \frac{V_{\mathbf{x},\mathbf{y}}(\alpha,\ldots,\alpha,\beta,\ldots,\beta)}{1+V_{\mathbf{x},\mathbf{y}}(\alpha,\ldots,\alpha,\beta,\ldots,\beta)} - c(\alpha,\beta)$$

with

$$c(\alpha,\beta) = \frac{1}{2}\left(\frac{V_{\mathbf{x}}(1,\ldots,1)}{\alpha+V_{\mathbf{x}}(1,\ldots,1)} + \frac{V_{\mathbf{y}}(1,\ldots,1)}{\beta+V_{\mathbf{y}}(1,\ldots,1)}\right),$$

where

$$V_{\mathbf{x},\mathbf{y}}(z_1,\ldots,z_k,z_{k+1},\ldots,z_{k+s}) = -\ln G_{\mathbf{x},\mathbf{y}}(z_1,\ldots,z_k,z_{k+1},\ldots,z_{k+s})$$

and

$$G_{\mathbf{x},\mathbf{y}}(z_1,\ldots,z_{k+s}) = P\left(\left\{\bigcap_{i=1}^{k}\{Z_{\mathbf{x}_i}\le z_i\}\right\}\bigcap\left\{\bigcap_{i=1}^{s}\{Z_{\mathbf{y}_i}\le z_{k+i}\}\right\}\right), \quad z_i\in\mathbb{R}^+.$$

Remark 2.6. For each $\alpha,\ \beta>0$ the coefficient $c(\alpha,\beta)$ considers the dependence intra each of the regions $\mathbf{x}$ and $\mathbf{y}$ through the extremal coefficients of vectors with margins $Z_{\boldsymbol{x}_1},\ldots,Z_{\boldsymbol{x}_k}$ and $Z_{\boldsymbol{y}_1},\ldots,Z_{\boldsymbol{y}_s}$. Therefore $\nu^{\alpha,\beta}(\mathbf{x},\mathbf{y})$ considers not only dependence inter regions but also intra regions. When we consider $c(\alpha,\beta)$ constant, the dependence between $\mathbf{x}$ and $\mathbf{y}$ is stronger for lower values of $\nu^{\alpha,\beta}(\mathbf{x},\mathbf{y})$, corresponding to lower values of $V_{\mathbf{x},\mathbf{y}}(\alpha,\ldots,\alpha,\beta,\ldots,\beta)$.

In the following proposition we establish some properties of the generalized madogram.

Proposition 2.7. Let $\mathbf{x} = \{\mathbf{x}_1,\ldots,\mathbf{x}_k\}$ and $\mathbf{y} = \{\mathbf{y}_1,\ldots,\mathbf{y}_s\}$ be disjoint regions of $\mathbb{R}^2$. We have, for each $\alpha,\beta\in\mathbb{R}^+$,

1. $0\le\nu^{\alpha,\beta}(\mathbf{x},\mathbf{y})\le\frac{1}{2}$;
2. $\nu^{\alpha,\alpha}(\mathbf{x},\mathbf{y}) = \frac{\epsilon_{\mathbf{x}\cup\mathbf{y}}}{\alpha+\epsilon_{\mathbf{x}\cup\mathbf{y}}} - \frac{1}{2}\left(\frac{\epsilon_{\mathbf{x}}}{\alpha+\epsilon_{\mathbf{x}}}+\frac{\epsilon_{\mathbf{y}}}{\alpha+\epsilon_{\mathbf{y}}}\right)$, where $\epsilon_{\mathbf{x}\cup\mathbf{y}} = V_{\mathbf{x},\mathbf{y}}(1,\ldots,1)$.

Remark 2.8. The function $\nu^{\alpha,\alpha}(\mathbf{x},\mathbf{y})$ can also be related with the dependence coefficients considered in Ferreira [7] as follows:

$$\nu^{\alpha,\alpha}(\mathbf{x},\mathbf{y}) = \frac{\epsilon_{\mathbf{y}}\epsilon_1(\mathbf{x},\mathbf{y})}{\alpha+\epsilon_{\mathbf{y}}\epsilon_1(\mathbf{x},\mathbf{y})} - c(\alpha,\alpha) = \frac{(\epsilon_{\mathbf{y}}+\epsilon_{\mathbf{x}})\epsilon_2(\mathbf{x},\mathbf{y})}{\alpha+(\epsilon_{\mathbf{y}}+\epsilon_{\mathbf{x}})\epsilon_2(\mathbf{x},\mathbf{y})} - c(\alpha,\alpha),\ \ \alpha>0,$$

where $\epsilon_1(\mathbf{x},\mathbf{y}) = \dfrac{\epsilon_{\mathbf{x}\cup\mathbf{y}}}{\epsilon_{\mathbf{y}}}$ and $\epsilon_2(\mathbf{x},\mathbf{y}) = \dfrac{\epsilon_{\mathbf{x}\cup\mathbf{y}}}{\epsilon_{\mathbf{x}}+\epsilon_{\mathbf{y}}}$. These coefficients evaluate the strength of dependence between the events $\{M(\mathbf{x})\le u\}$ and $\{M(\mathbf{y})\le u\}$.

Remark 2.9. If the variables $M(\mathbf{x})$ and $M(\mathbf{y})$ are independent then

$$\nu^{\alpha,\alpha}(\mathbf{x},\mathbf{y}) = \frac{\epsilon_{\mathbf{x}}+\epsilon_{\mathbf{y}}}{\alpha+\epsilon_{\mathbf{x}}+\epsilon_{\mathbf{y}}} - \frac{1}{2}\left(\frac{\epsilon_{\mathbf{x}}}{\alpha+\epsilon_{\mathbf{x}}}+\frac{\epsilon_{\mathbf{y}}}{\alpha+\epsilon_{\mathbf{y}}}\right),$$

whereas if they are totally dependent

$$\nu^{\alpha,\alpha}(\mathbf{x},\mathbf{y}) = \frac{\epsilon_{\mathbf{x}}\vee\epsilon_{\mathbf{y}}}{\alpha+\epsilon_{\mathbf{x}}\vee\epsilon_{\mathbf{y}}} - \frac{1}{2}\left(\frac{\epsilon_{\mathbf{x}}}{\alpha+\epsilon_{\mathbf{x}}}+\frac{\epsilon_{\mathbf{y}}}{\alpha+\epsilon_{\mathbf{y}}}\right).$$

3. ESTIMATING THE GENERALIZED MADOGRAM

Proposition 2.1 relates the generalized madogram with well known dependence measures. Immediate estimators for the generalized madogram can then be obtained through the estimators of those measures, which have already been studied in the literature. For a survey we refer to Krajina [9], Beirlant et al. [1] and Schlather and Tawn [15].

In this section we present a natural non-parametric estimator for the generalized madogram based on sample means.

Let $(Z^{(t)}_{\boldsymbol{x}_1},\dots,Z^{(t)}_{\boldsymbol{x}_k})$ and $(Z^{(t)}_{\boldsymbol{y}_1},\dots,Z^{(t)}_{\boldsymbol{y}_s})$, $t=1,\dots,T$, be independent replications of $(Z_{\boldsymbol{x}_1},\dots,Z_{\boldsymbol{x}_k})$ and $(Z_{\boldsymbol{y}_1},\dots,Z_{\boldsymbol{y}_s})$, respectively. Hence $\{M_t(\mathbf{x}) = \bigvee_{i=1}^{k} Z^{(t)}_{\boldsymbol{x}_i},\ t=1,\dots,T\}$ and $\{M_t(\mathbf{y}) = \bigvee_{i=1}^{s} Z^{(t)}_{\boldsymbol{y}_i},\ t=1,\dots,T\}$ are random samples of $M(\mathbf{x})$ and $M(\mathbf{y})$, respectively.

In the case of known marginal distribution $F_{\boldsymbol{x}_i}$ of $Z_{\boldsymbol{x}_i}$, which becomes unit Fréchet by transformation $-\frac{1}{\log F_{\boldsymbol{x}_i}(Z_{\boldsymbol{x}_i})}$ for $\boldsymbol{x}_i\in\mathbb{R}^2$, the estimator for the generalized madogram is given by

$$\widehat{\nu}^{\alpha,\beta}(\mathbf{x},\mathbf{y}) = \frac{1}{2T}\sum_{t=1}^{T}|F^{\alpha}(M_t(\mathbf{x})) - F^{\beta}(M_t(\mathbf{y}))|, \quad \alpha>0,\ \beta>0.$$

This estimator is unbiased and converges in distribution to a Gaussian distribution, as stated in the following proposition.

Proposition 3.1. (Asymptotic normality and strong consistency under known marginal distribution F)

We have

$$\frac{\sqrt{T}(\widehat{\nu}^{\alpha,\beta}(\mathbf{x},\mathbf{y}) - \nu^{\alpha,\beta}(\mathbf{x},\mathbf{y}))}{\sigma} \to N(0,1),$$

where $\sigma^2 = \frac{1}{2}\gamma_F^{\alpha,\beta}(\mathbf{x},\mathbf{y}) - (\nu^{\alpha,\beta}(\mathbf{x},\mathbf{y}))^2$ and $\gamma_F^{\alpha,\beta}(\mathbf{x},\mathbf{y}) = \frac{1}{2}E\left[(F^{\alpha}(M(\mathbf{x})) - F^{\beta}(M(\mathbf{y})))^2\right]$. Moreover, $\widehat{\nu}^{\alpha,\beta}(\mathbf{x},\mathbf{y})$ converges almost surely to $\nu^{\alpha,\beta}(\mathbf{x},\mathbf{y})$.

When the distribution of each $Z_{\boldsymbol{x}_i}$, $F_{\boldsymbol{x}_i}$, is unknown we take the empirical Fréchet normalization of the variables, i. e., $\widehat{U}^{(t)}_{\boldsymbol{x}_i} = -\frac{1}{\log(\widehat{F}_{\boldsymbol{x}_i}(Z^{(t)}_{\boldsymbol{x}_i}))}$, where $\widehat{F}_{\boldsymbol{x}_i}$ is the empirical

distribution function. We then find the following modification of the above estimator

$$\begin{aligned}
\widehat{\widehat{\nu}}^{\alpha,\beta}(\mathbf{x},\mathbf{y}) &= \frac{1}{2T}\sum_{t=1}^{T}\left|F^{\alpha}\left(\bigvee_{i=1}^{k}\widehat{U}^{(t)}_{\boldsymbol{x}_i}\right)-F^{\beta}\left(\bigvee_{j=1}^{s}\widehat{U}^{(t)}_{\boldsymbol{y}_j}\right)\right| \\
&= \frac{1}{2T}\sum_{t=1}^{T}\left|\bigvee_{i=1}^{k}F\left(\frac{\widehat{U}^{(t)}_{\boldsymbol{x}_i}}{\alpha}\right)-\bigvee_{j=1}^{s}F\left(\frac{\widehat{U}^{(t)}_{\boldsymbol{y}_j}}{\beta}\right)\right| \\
&= \frac{1}{2T}\sum_{t=1}^{T}\left|\bigvee_{i=1}^{k}\widehat{F}^{\alpha}_{\boldsymbol{x}_i}\left(Z^{(t)}_{\boldsymbol{x}_i}\right)-\bigvee_{j=1}^{s}\widehat{F}^{\beta}_{\boldsymbol{y}_j}\left(Z^{(t)}_{\boldsymbol{y}_j}\right)\right|, \quad \alpha>0,\ \beta>0, \qquad (4)
\end{aligned}$$

where

$$\widehat{F}_{\boldsymbol{x}_i}(u)=\frac{1}{T}\sum_{t=1}^{T}\mathbb{1}_{\{Z^{(t)}_{\boldsymbol{x}_i}\le u\}}.$$

Proposition 3.2. The estimator $\widehat{\widehat{\nu}}^{\alpha,\beta}(\mathbf{x},\mathbf{y})$, defined in (4), is strongly consistent.

The asymptotic normality of the estimator is obtained by considering

$$J(x_1,\ldots,x_{k+s})=\frac{1}{2}\left|\bigvee_{i=1}^{k}x_i^{\alpha}-\bigvee_{i=k+1}^{k+s}x_i^{\beta}\right|$$

in the following theorem stated in Fermanian *et al.* [6]. Such a function is of bounded variation, continuous from above and with discontinuities of the first kind (Neuhaus [11]).

Theorem 3.3. Let $(Z_{\mathbf{x}_1},\ldots,Z_{\mathbf{x}_k},Z_{\mathbf{y}_1},\ldots,Z_{\mathbf{y}_s})$ be a random vector with d.f. H and continuous marginal d.f.'s $F_{\mathbf{x}_1},\ldots,F_{\mathbf{x}_k},F_{\mathbf{y}_1},\ldots,F_{\mathbf{y}_s}$ and let the copula associated to H, C_H, have continuous partial derivatives. Assume that $J:[0,1]^{k+s}\to\mathbb{R}$ is of bounded variation, continuous from above and with discontinuities of the first kind. Then, as $T\to\infty$,

$$\begin{aligned}
&\frac{1}{\sqrt{T}}\sum_{i=1}^{T}\Big\{J(\widehat{F}_{\mathbf{x}_1}(Z^{(i)}_{\mathbf{x}_1}),\ldots,\widehat{F}_{\mathbf{x}_k}(Z^{(i)}_{\mathbf{x}_k}),\widehat{F}_{\mathbf{y}_1}(Z^{(i)}_{\mathbf{y}_1}),\ldots,\widehat{F}_{\mathbf{y}_s}(Z^{(i)}_{\mathbf{y}_s})) \\
&\qquad -E(J(F_{\mathbf{x}_1}(Z^{(i)}_{\mathbf{x}_1}),\ldots,F_{\mathbf{x}_k}(Z^{(i)}_{\mathbf{x}_k}),F_{\mathbf{y}_1}(Z^{(i)}_{\mathbf{y}_1}),\ldots,F_{\mathbf{y}_s}(Z^{(i)}_{\mathbf{y}_s})))\Big\} \\
&\to \int_{[0,1]^{k+s}}\mathbb{G}(u_1,\ldots,u_{k+s})\,\mathrm{d}J(u_1,\ldots,u_{k+s}),
\end{aligned}$$

in distribution in $l^{\infty}\left([0,1]^{k+s}\right)$ where the limiting process and $\mathbb{G}$ are centered Gaussian.

In the following section we will conduct a simulation study of an M4 random field to assess the performance of the estimator $\widehat{\widehat{\nu}}^{\alpha,\beta}_{\mathbf{x},\mathbf{y}}$.

4. AN M4 RANDOM FIELD

It is well known that the class of max-stable processes called multivariate maxima of moving maxima processes or simply M4 processes, introduced by Smith and Weissman [17], is particularly well adapted to modeling the extreme behaviour of several time series (Zhang and Smith [20, 21]).

To illustrate the computation of the generalized madogram given in (4) we will now define an M4 random field.

Let us consider that the distribution of $(Z_{\boldsymbol{x}_1}, \ldots, Z_{\boldsymbol{x}_p})$ is characterized by the copula

$$C(u_{\boldsymbol{x}_1}, \ldots, u_{\boldsymbol{x}_p}) = \prod_{l=1}^{+\infty} \prod_{m=-\infty}^{+\infty} \bigwedge_{\boldsymbol{x} \in \{\boldsymbol{x}_1, \ldots, \boldsymbol{x}_p\}} u_{\boldsymbol{x}}^{a_{lm\boldsymbol{x}}}, \quad u_{\boldsymbol{x}_i} \in [0,1],\ i = 1, \ldots, p, \tag{5}$$

where, for each $\boldsymbol{x} \in \mathbb{Z}^2$, $\{a_{lm\boldsymbol{x}}\}_{l \geq 1, m \in \mathbb{Z}}$ are non-negative constants such that $\sum_{l=1}^{+\infty} \sum_{m=-\infty}^{+\infty} a_{lm\boldsymbol{x}} = 1$. This random field $\mathbf{Z}$ is max-stable, since, for each $t > 0$, the copula (5) satisfies

$$C^t(u_{\boldsymbol{x}_1}, \ldots, u_{\boldsymbol{x}_p}) = C(u_{\boldsymbol{x}_1}^t, \ldots, u_{\boldsymbol{x}_p}^t),$$

for any locations $\boldsymbol{x}_1, \ldots, \boldsymbol{x}_p$.

As the M4 process considered in Smith and Weissman [17], we can consider that for each location $\boldsymbol{x}$, $Z_{\boldsymbol{x}}$ is a moving maxima of variables $X_{l,n}$, i. e.,

$$Z_{\boldsymbol{x}} = \max_{l \geq 1} \max_{-\infty < m < +\infty} a_{lm\boldsymbol{x}} X_{l,1-m}, \quad \boldsymbol{x} \in \mathbb{Z}^2, \tag{6}$$

where $\{X_{l,n}\}_{l \geq 1, n \in \mathbb{Z}}$ is a family of independent unit Fréchet random variables. The dependence structure of $(Z_{\boldsymbol{x}_1}, \ldots, Z_{\boldsymbol{x}_p})$ is regulated by the signatures patterns $a_{lm\boldsymbol{x}}$ and is given by (5).

For each pair of regions $\mathbf{x} = \{\boldsymbol{x}_1, \ldots, \boldsymbol{x}_k\}$ and $\mathbf{y} = \{\boldsymbol{y}_{k+1}, \ldots, \boldsymbol{y}_{k+s}\}$ we have

$$\begin{aligned} & V_{\mathbf{x},\mathbf{y}}(z_1, \ldots, z_k, z_{k+1}, \ldots, z_{k+s}) \\ = \ & -\ln C(e^{-z_1^{-1}}, \ldots, e^{-z_{k+s}^{-1}}) \\ = \ & \sum_{l=1}^{+\infty} \sum_{m=-\infty}^{+\infty} \bigvee_{i=1}^{k} z_i^{-1} a_{lm\boldsymbol{x}_i} \vee \bigvee_{i=k+1}^{s} z_i^{-1} a_{lm\boldsymbol{y}_i},\ z_i \in \mathbb{R},\ i = 1, \ldots, k+s, \end{aligned}$$

and consequently, for $\alpha > 0$ and $\beta > 0$ we obtain

$$V_{\mathbf{x},\mathbf{y}}(\alpha, \ldots, \alpha, \beta, \ldots, \beta) = \sum_{l=1}^{+\infty} \sum_{m=-\infty}^{+\infty} \left(\bigvee_{i=1}^{k} \alpha^{-1} a_{lm\boldsymbol{x}_i} \vee \bigvee_{i=k+1}^{k+s} \beta^{-1} a_{lm\boldsymbol{y}_i} \right).$$

To illustrate the computation of the generalized madogram we shall consider, in what follows, examples with a finite number of signature patterns ($1 \leq l \leq L$) and a finite range of sequential dependencies ($M_1 \leq m \leq M_2$).

Example 4.1. Let us consider that for each location $\boldsymbol{x} \in \mathbb{Z}^2$ with even coordinates we have $a_{11\boldsymbol{x}} = a_{12\boldsymbol{x}} = \frac{1}{2}$ and otherwise $a_{11\boldsymbol{x}} = \frac{1}{4} = 1 - a_{12\boldsymbol{x}}$ (Figure 1). The values of $(a_{11\boldsymbol{x}}, a_{12\boldsymbol{x}})$ determine the moving pattern or signature pattern of the random field, which in this case corresponds to one pattern ($L = 1$).

For the disjoint regions of locations $\mathbf{x} = \{(2,1),(2,2)\}$ and $\mathbf{y} = \{(2,3),(3,3)\}$ we have

$$V_{\mathbf{x},\mathbf{y}}(\alpha,\alpha,\beta,\beta) = \frac{1}{4}(2\alpha^{-1} \vee \beta^{-1}) + \frac{3}{4}(\alpha^{-1} \vee \beta^{-1})$$

and therefore, the generalized madogram in this pair of locations is given by

$$\nu^{\alpha,\beta}(\mathbf{x},\mathbf{y}) = \frac{\frac{1}{4}(2\alpha^{-1} \vee \beta^{-1}) + \frac{3}{4}(\alpha^{-1} \vee \beta^{-1})}{1 + \frac{1}{4}(2\alpha^{-1} \vee \beta^{-1}) + \frac{3}{4}(\alpha^{-1} \vee \beta^{-1})} - \frac{1}{2}\left(\frac{\frac{5}{4}}{\alpha + \frac{5}{4}} + \frac{1}{\beta + 1}\right), \quad \alpha > 0,\ \beta > 0.$$

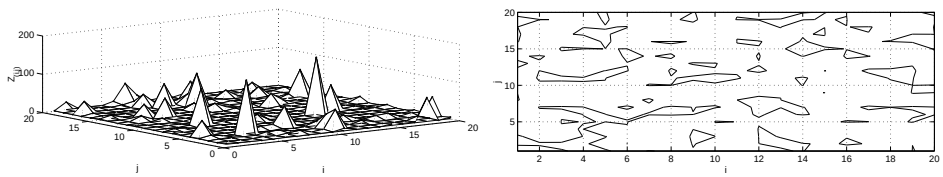

Fig. 1. Simulation of the M4 as defined in Example 4.1 (left) and the contour at $z_{(i,j)} = 21.1507$, the 95% quantile, (right).

Example 4.2. As stated in Zhang and Smith [20], in a real data generating process it is unrealistic to assume that a single signature pattern would be sufficient to describe the shape of the process every time it exceeds some high threshold. Hence, we shall now consider one example with two signature patterns ($L = 2$).

Let us assume that for each location $\boldsymbol{x} = (i,j)$ we have $a_{11\boldsymbol{x}} = a_{12\boldsymbol{x}} = a_{13\boldsymbol{x}} = \frac{1}{12}$, $a_{21\boldsymbol{x}} = a_{22\boldsymbol{x}} = a_{23\boldsymbol{x}} = \frac{1}{4}$ if both coordinates are odd and $a_{11\boldsymbol{x}} = \frac{1}{18}$, $a_{12\boldsymbol{x}} = \frac{1}{9}$, $a_{13\boldsymbol{x}} = \frac{1}{6}$, $a_{21\boldsymbol{x}} = a_{22\boldsymbol{x}} = a_{23\boldsymbol{x}} = \frac{2}{9}$ otherwise. Now the values of $(a_{11\boldsymbol{x}}, a_{12\boldsymbol{x}}, a_{13\boldsymbol{x}})$ and $(a_{21\boldsymbol{x}}, a_{22\boldsymbol{x}}, a_{23\boldsymbol{x}})$ define the two signature patterns of the random field (Figure 2).

For the two disjoint regions previously considered $\mathbf{x} = \{(2,1),(2,2)\}$ and $\mathbf{y} = \{(2,3),(3,3)\}$ we now have

$$V_{\mathbf{x},\mathbf{y}}(\alpha,\alpha,\beta,\beta) = \left(\alpha^{-1}\frac{1}{18} \vee \beta^{-1}\frac{1}{12}\right) + \frac{1}{9}\left(\alpha^{-1} \vee \beta^{-1}\right) + \frac{1}{6}\left(\alpha^{-1} \vee \beta^{-1}\right) + \left(\alpha^{-1}\frac{2}{3} \vee \beta^{-1}\frac{3}{4}\right)$$

and consequently

$$\begin{aligned}\nu^{\alpha,\beta}(\mathbf{x},\mathbf{y}) \quad = \quad & \frac{\left(\frac{\alpha^{-1}}{18} \vee \frac{\beta^{-1}}{12}\right) + \frac{(\alpha^{-1} \vee \beta^{-1})}{9} + \frac{(\alpha^{-1} \vee \beta^{-1})}{6} + \left(\frac{2\alpha^{-1}}{3} \vee \frac{3\beta^{-1}}{4}\right)}{1 + \left(\frac{\alpha^{-1}}{18} \vee \frac{\beta^{-1}}{12}\right) + \frac{(\alpha^{-1} \vee \beta^{-1})}{9} + \frac{(\alpha^{-1} \vee \beta^{-1})}{6} + \left(\frac{2\alpha^{-1}}{3} \vee \frac{3\beta^{-1}}{4}\right)} \\ & - \frac{1}{2}\left(\frac{1}{\alpha + 1} + \frac{\frac{10}{9}}{\beta + \frac{10}{9}}\right), \quad \alpha > 0,\ \beta > 0.\end{aligned}$$

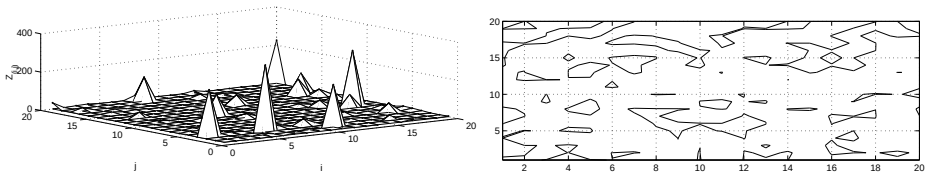

Fig. 2. Simulation of the M4 random field as defined in Example 4.2 (left) and the contour at $z_{(i,j)} = 26.5302$, the 95% quantile, (right).

These examples will be used in the following simulation studies to assess the performance of the estimator given in (4). Figures 3 and 5 show the simulation results obtained by generating 50 replications of 100 independently and identically distributed max-stable M4 random fields in the two situations previously presented, with α and β taking values in $\{0.2, 0.4, 0.6, 0.8, 1, 2, 3, \ldots, 20\}$. To better illustrate the performance of our estimator we present in Figures 4 and 6 the true and mean estimated values of the generalized madogram for some $\alpha, \beta > 0$.

As we can see from the values of the mean square error (Figures 3 and 5) the estimates obtained from our estimator $\widehat{\widehat{\nu}}^{\alpha,\beta}(\mathbf{x}, \mathbf{y})$ are quite close to the true values of the generalized madogram. Figures 4 and 6 highlight the good performance of our estimator. For an M4 random field with one signature pattern values of $\alpha = \beta$ seem to lead to the worst estimates of the generalized madogram, whereas for two signature patterns the worst estimates are obtained when $\beta > 10$ and $\alpha < \beta$.

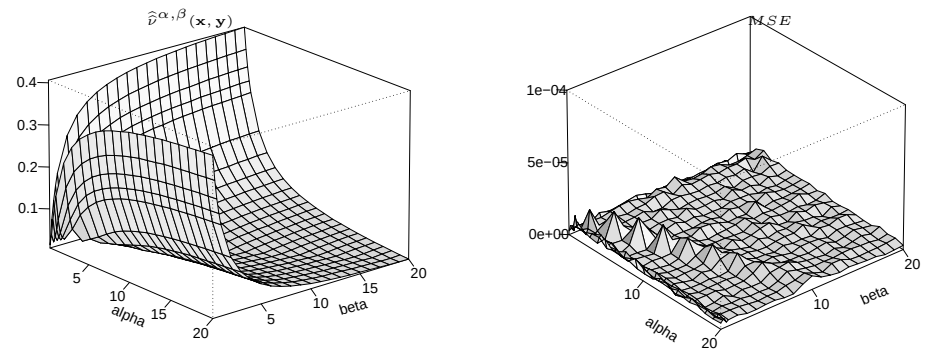

Fig. 3. The mean estimated values of the generalized madogram ($\widehat{\widehat{\nu}}^{\alpha,\beta}(\mathbf{x}, \mathbf{y})$) and the estimated mean squared error (MSE) for Example 4.1 with $\alpha, \beta \in \{0.2, 0.4, 0.6, 0.8, 1, 2, 3, \ldots, 20\}$.

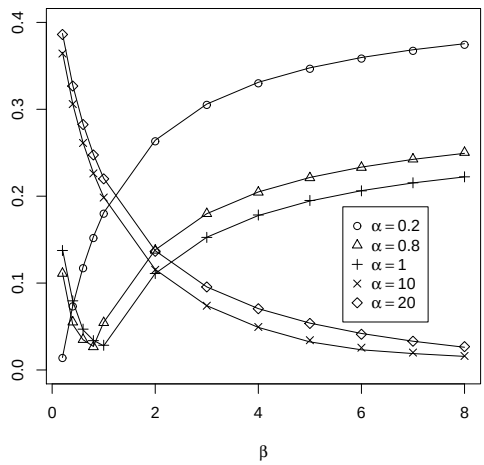

Fig. 4. The solid line represents true values of generalized madogram ($\nu^{\alpha,\beta}(\mathbf{x},\mathbf{y})$) and points represent the mean estimated values ($\widehat{\widehat{\nu}}^{\alpha,\beta}(\mathbf{x},\mathbf{y})$) for Example 4.1, with $\alpha \in \{0.2, 0.8, 1, 10, 20\}$ and $\beta \in \{0.2, 0.4, 0.6, 0.8, 1, 2, 3, 4, 5, 6, 7, 8\}$.

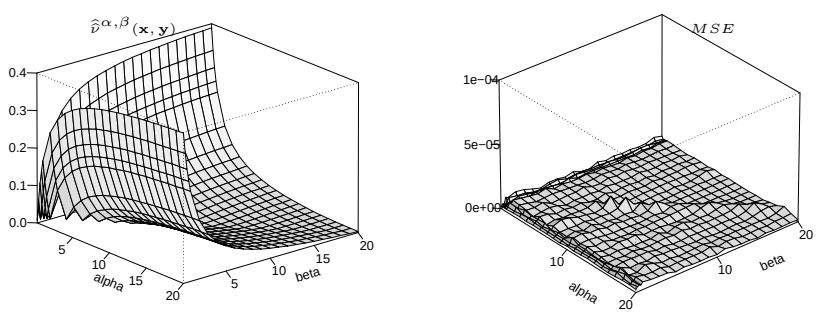

Fig. 5. The mean estimated values of the generalized madogram ($\widehat{\widehat{\nu}}^{\alpha,\beta}(\mathbf{x},\mathbf{y})$) and the estimated mean squared error (MSE) for Example 4.2 with $\alpha, \beta \in \{0.2, 0.4, 0.6, 0.8, 1, 2, 3, \ldots, 20\}$.

5. APPLICATION TO PRECIPITATION DATA

We now consider an application of the proposed estimator of the generalized madogram to annual maxima values of daily maxima rainfall in different topographic regions of Portugal.

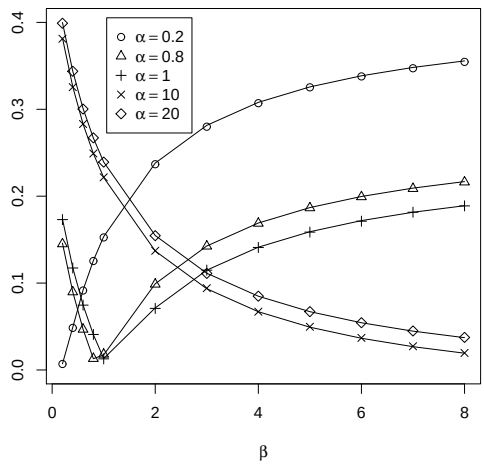

Fig. 6. The solid line represents true values of generalized madogram ($\nu^{\alpha,\beta}(\mathbf{x},\mathbf{y})$) and points represent the mean estimated values ($\widehat{\widehat{\nu}}^{\alpha,\beta}(\mathbf{x},\mathbf{y})$) for Example 4.2, with $\alpha \in \{0.2, 0.8, 1, 10, 20\}$ and $\beta \in \{0.2, 0.4, 0.6, 0.8, 1, 2, 3, 4, 5, 6, 7, 8\}$.

In Portugal there are topographic differences between north and south, whereas in the north there are several mountains, in the south there are mainly plateaus and plains. The Central Cordillera, formed by the mountains of Sintra, Montejunto and Estrela, divides south and north and influences climate in Portugal, namely precipitation. The majority of the precipitation in Portugal comes from North-West and it is more abundant in the north than in the south due to the Central Cordillera that creates a physical barrier for precipitation.

To study the dependence between extreme precipitation occurring in this mountain area and in surrounding areas, we considered precipitation data that consist of annual maxima of daily maxima precipitation recorded over 32 years (between 1944 and 1981), in 5 Portuguese stations, obtained from the Portuguese National System of Water Resources (http://snirh.pt). In Figure 7 we can view the location of the 5 stations considered. We remark that the stations "Lagoa Comprida" and "Fajão" are located in North-West part of "Serra da Estrela", the highest mountain in continental Portugal and part of the Central Cordillera.

Since the data are maxima over a long period of time, we assumed that they are independent over the years in each location. We also assumed that the random field is max-stable with unknown marginal distributions, so data were previously transformed at each site to become standard Fréchet distribution.

In Figures 8, 9 and 10 we picture the estimated values of the generalized madogram, for several values of α and β, when considering the mountain region $\mathbf{x} = \{\text{Fajão, L. Comprida}\}$ and different topographic surrounding regions, that are either to north or to the south of this region.

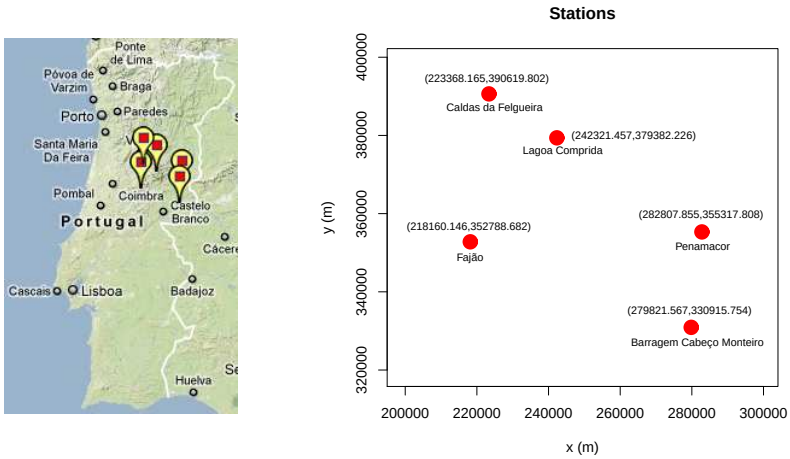

Fig. 7. The locations of the stations where precipitation data were collected, obtained from Portuguese National System of Water Resources (left) and their representation in Lambert coordinates (right).

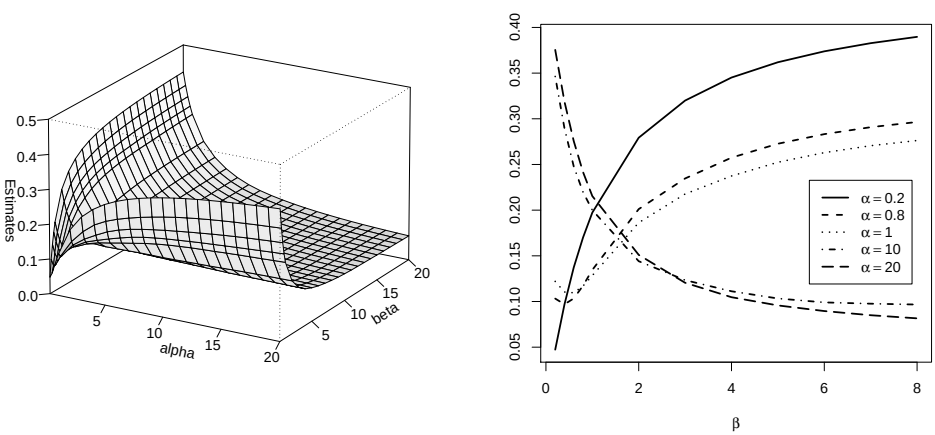

Fig. 8. Generalized madogram ($\widehat{\nu}^{\alpha,\beta}(\mathbf{x},\mathbf{y})$) estimates obtained for $\mathbf{x} = \{\text{L. Comprida,Fajão}\}$, $\mathbf{y} = \{\text{B.C.M.}\}$ with $\alpha, \beta \in \{0.2, 0.4, 0.6, 0.8, 1, 2, 3, \ldots, 20\}$, on the left, and for $\alpha \in \{0.2, 0.8, 1, 10, 20\}$ and $\beta \in \{0.2, 0.4, 0.6, 0.8, 1, 2, 3, 4, 5, 6, 7, 8\}$, on the right.

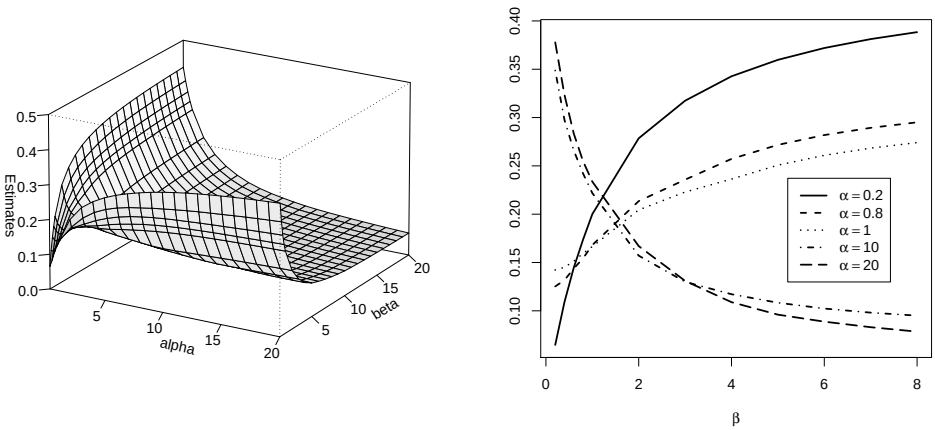

Fig. 9. Generalized madogram ($\widehat{\widehat{\nu}}^{\alpha,\beta}(\mathbf{x},\mathbf{y})$) estimates obtained for $\mathbf{x} = \{\text{L. Comprida,Fajão}\}$, $\mathbf{y} = \{\text{Penamacor}\}$ with $\alpha, \beta \in \{0.2, 0.4, 0.6, 0.8, 1, 2, 3, \ldots, 20\}$, on the left, and for $\alpha \in \{0.2, 0.8, 1, 10, 20\}$ and $\beta \in \{0.2, 0.4, 0.6, 0.8, 1, 2, 3, 4, 5, 6, 7, 8\}$, on the right.

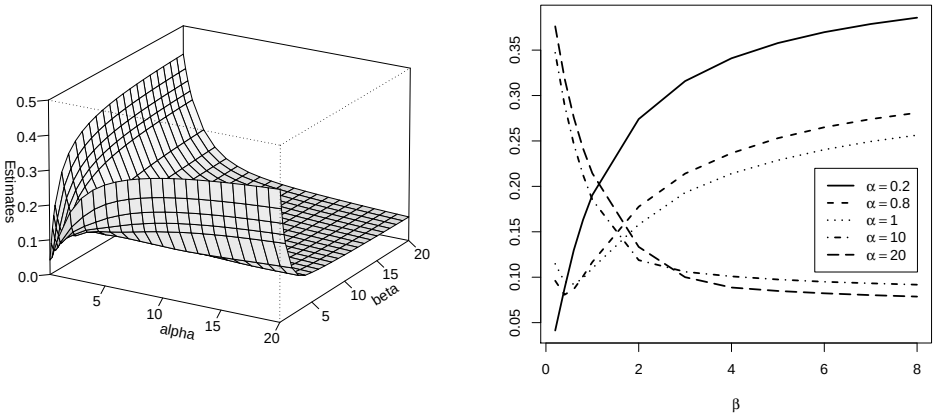

Fig. 10. Generalized madogram ($\widehat{\widehat{\nu}}^{\alpha,\beta}(\mathbf{x},\mathbf{y})$) estimates obtained for $\mathbf{x} = \{\text{L. Comprida,Fajão}\}$, $\mathbf{y} = \{\text{C. Felgueira}\}$ with $\alpha, \beta \in \{0.2, 0.4, 0.6, 0.8, 1, 2, 3, \ldots, 20\}$, on the left, and for $\alpha \in \{0.2, 0.8, 1, 10, 20\}$ and $\beta \in \{0.2, 0.4, 0.6, 0.8, 1, 2, 3, 4, 5, 6, 7, 8\}$, on the right.

Since there is not a reason to take different weights for the considered locations, in the following we take $\alpha = \lambda/k$ and $\beta = (1-\lambda)/s$, $\lambda \in (0,1)$, where k and s are the number of locations in region $\mathbf{x}$ and $\mathbf{y}$, respectively, as stated in Remark 3. The estimated values for this particular choice of α and β are presented in Figure 11.

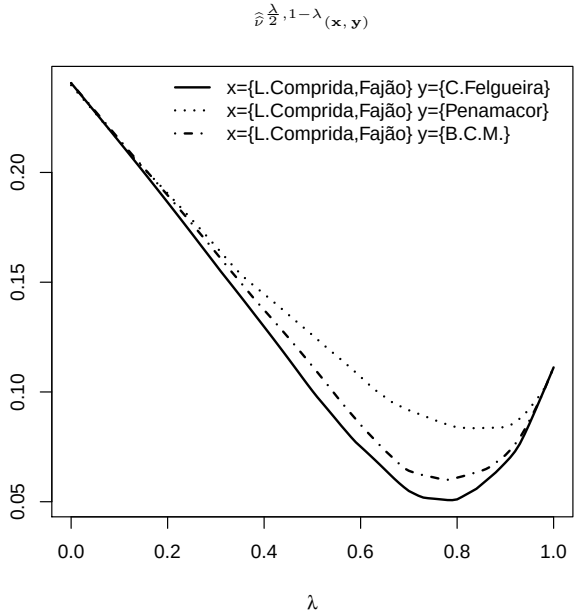

Fig. 11. Generalized madogram ($\widehat{\nu}^{\alpha,\beta}(\mathbf{x},\mathbf{y})$) estimates obtained for each pair of disjoint regions when $\alpha = \frac{\lambda}{2}$ and $\beta = 1-\lambda$ with $\lambda \in (0,1)$.

Since lower values for $\nu^{\alpha,\beta}(\mathbf{x},\mathbf{y})$ indicate strong dependence, the results presented in Figure 11 suggest a stronger dependence between the mountain region $\mathbf{x} = \{\text{Fajão, L. Comprida}\}$ and the north region $\mathbf{y} = \{\text{C. Felgueira}\}$. This is in accordance with the previously stated that the Central Cordillera creates a physical barrier for precipitation in Portugal.

Considering the estimated values of the λ-madogram for the pairs of locations (L. Comprida, C. Felgueira) and (Fajão, C. Felgueira) and the estimates of the generalized madogram for regions $\mathbf{x} = \{\text{Fajão, L. Comprida}\}$ and $\mathbf{y} = \{\text{C. Felgueira}\}$ we obtained, as expected, different patterns (Figure 12), since the generalized madogram considers not only the dependence inter regions but also intra regions.

It would be interesting to further investigate this dependence with other regions but the lack of available data restricts the possible regions to study.

6. CONCLUSION

In this work we presented a new dependence coefficient called generalized madogram which extends the λ-madogram. The advantage of this measure is that it allows the

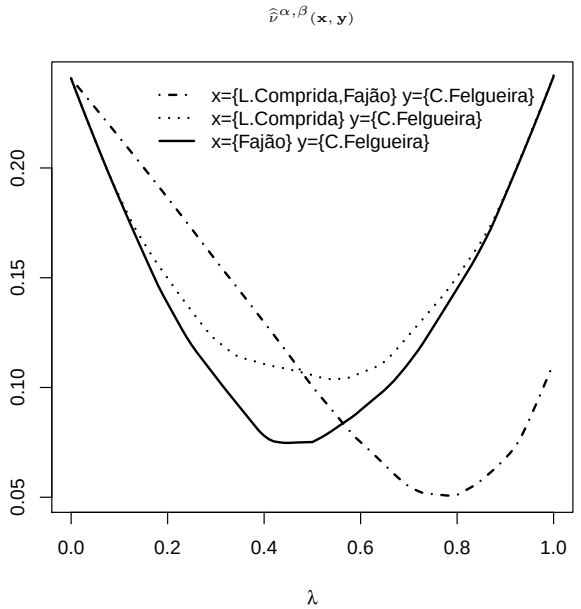

Fig. 12. Generalized madogram ($\widehat{\widehat{\nu}}^{\alpha,\beta}(\mathbf{x},\mathbf{y})$) estimates obtained for $\mathbf{x} = \{\text{L. Comprida,Fajão}\}$, $\mathbf{y} = \{\text{C. Felgueira}\}$ when $\alpha = \frac{\lambda}{2}$ and $\beta = 1 - \lambda$ with $\lambda \in (0, 1)$ and λ-madogram estimates for the other regions.

assessment of dependence between maxima over two disjoint regions of locations, incorporating dependence inter and intra regions. Besides the theoretical study of this coefficient, estimators were proposed and a simulation study was carried out to evaluate its behavior. Applications to real data were also presented. The simulation results show the good performance of the proposed estimator for the generalized madogram, when considering an M4 random field. The results obtained in the application to precipitation data from Portuguese regions are in accordance with the expected dependence in this case, enhancing the practical utility of the proposed coefficient.

All the simulations presented in this paper were done in R statistical computing program (http://cran.r-project. org/). We remark that several packages on Extreme Value analysis have been recently introduced into R, but more recently Ribatet [13] added to R the package SpatialExtremes that provides functions to analyze and fit max-stable processes to spatial extremes.

ACKNOWLEDGEMENT

We are grateful to the referees for their detailed comments and suggestions which helped the final form of this paper. This research was supported by the research projects PTDC/MAT/108575/2008 and PEst-OE/MAT/UI0212/2014.

Appendix

Proof of Proposition 2.5

To obtain the result, we start by transforming the definition of $\nu^{\alpha,\beta}(\mathbf{x},\mathbf{y})$ through the relation $|a-b| = 2(a \vee b) - (a+b)$, and then take into account that

$$E\left(F^{\alpha}\left(M(\mathbf{x})\right) \vee F^{\beta}\left(M(\mathbf{y})\right)\right) = E\left(F\left(\frac{M(\mathbf{x})}{\alpha} \vee \frac{M(\mathbf{y})}{\beta}\right)\right)$$

and

$$\begin{aligned} P\left(\frac{M(\mathbf{x})}{\alpha} \vee \frac{M(\mathbf{y})}{\beta} \leq u\right) &= P\left(M(\mathbf{x}) \leq \alpha u, M(\mathbf{y}) \leq \beta u\right) \\ &= G_{\mathbf{x},\mathbf{y}}(\alpha u, \ldots, \alpha u, \beta u, \ldots, \beta u) \\ &= \exp\left\{-u^{-1} V_{\mathbf{x},\mathbf{y}}(\alpha, \ldots, \alpha, \beta, \ldots, \beta)\right\}, \quad u > 0. \end{aligned}$$

Hence,

$$\begin{aligned} & E\left(F\left(\frac{M(\mathbf{x})}{\alpha} \vee \frac{M(\mathbf{y})}{\beta}\right)\right) \\ &= \int_0^{+\infty} F(u) \exp\left(-V_{\mathbf{x},\mathbf{y}}(\alpha u, \ldots, \alpha u, \beta u, \ldots, \beta u)\right) \\ &\qquad \frac{\mathrm{d}}{\mathrm{d}u}\left(-V_{\mathbf{x},\mathbf{y}}(\alpha u, \ldots, \alpha u, \beta u, \ldots, \beta u)\right) \mathrm{d}u \\ &= \int_0^{+\infty} \exp\left(-u^{-1} - u^{-1} V_{\mathbf{x},\mathbf{y}}(\alpha, \ldots, \alpha, \beta, \ldots, \beta)\right) u^{-2} V_{\mathbf{x},\mathbf{y}}(\alpha, \ldots, \alpha, \beta, \ldots, \beta)\, \mathrm{d}u \\ &= \frac{V_{\mathbf{x},\mathbf{y}}(\alpha, \ldots, \alpha, \beta, \ldots, \beta)}{1 + V_{\mathbf{x},\mathbf{y}}(\alpha, \ldots, \alpha, \beta, \ldots, \beta)}. \end{aligned}$$

Using similar arguments, we obtain $E\left(F^{\alpha}(M(\mathbf{x}))\right) = \frac{V_{\mathbf{x}}(\alpha,\ldots,\alpha)}{1+V_{\mathbf{x}}(\alpha,\ldots,\alpha)} = \frac{V_{\mathbf{x}}(1,\ldots,1)}{\alpha+V_{\mathbf{x}}(1,\ldots,1)}$ and $E\left(F^{\beta}(M(\mathbf{y}))\right) = \frac{V_{\mathbf{y}}(\beta,\ldots,\beta)}{1+V_{\mathbf{y}}(\beta,\ldots,\beta)} = \frac{V_{\mathbf{y}}(1,\ldots,1)}{\beta+V_{\mathbf{y}}(1,\ldots,1)}$. □

Proof of Proposition 2.7

The first statement results from the definition of the generalized madogram and the second follows from the definition of the extremal coefficient ϵ. □

Proof of Proposition 3.1

Let $Y_1, \ldots, Y_T$ be independent copies of $Y = \frac{1}{2}\left|F^{\alpha}(M(\mathbf{x})) - F^{\beta}(M(\mathbf{y}))\right|$. We have that

$$\frac{\sqrt{T}(\bar{Y} - \mu_Y)}{\sigma_Y} \to N(0,1),$$

where $\mu_Y = \frac{1}{2}E\left|F^\alpha(M(\mathbf{x})) - F^\beta(M(\mathbf{y}))\right| = \nu^{\alpha,\beta}(\mathbf{x},\mathbf{y})$ and $\sigma_Y^2 = \frac{1}{2}\gamma_F^{\alpha,\beta}(\mathbf{x},\mathbf{y}) - (\nu^{\alpha,\beta}(\mathbf{x},\mathbf{y}))^2$.

The strong consistency of $\widehat{\nu}^{\alpha,\beta}(\mathbf{x},\mathbf{y})$ follows since the sample mean converges almost surely to the mean value. □

P r o o f of Proposition 3.2

The estimator $\widehat{\widehat{\nu}}^{\alpha,\beta}(\mathbf{x},\mathbf{y})$ is strongly consistent since it holds

$$\left|\frac{1}{2}\frac{1}{T}\sum_{t=1}^{T}\left|\bigvee_{i=1}^{k}\widehat{F}_{\boldsymbol{x}_i}^{\alpha}\left(Z_{\boldsymbol{x}_i}^{(t)}\right) - \bigvee_{j=1}^{s}\widehat{F}_{\boldsymbol{y}_j}^{\beta}(Z_{\boldsymbol{y}_j}^{(t)})\right| - \frac{1}{2}E\left|\bigvee_{i=1}^{k}F^{\alpha}(Z_{\boldsymbol{x}_i}^{(t)}) - \bigvee_{j=1}^{s}F^{\beta}(Z_{\boldsymbol{y}_j}^{(t)})\right|\right|$$

$$\leq \left|\frac{1}{2}\frac{1}{T}\sum_{t=1}^{T}\left|\bigvee_{i=1}^{k}\widehat{F}_{\boldsymbol{x}_i}^{\alpha}\left(Z_{\boldsymbol{x}_i}^{(t)}\right) - \bigvee_{j=1}^{s}\widehat{F}_{\boldsymbol{y}_j}^{\beta}(Z_{\boldsymbol{y}_j}^{(t)})\right| - \frac{1}{2}\frac{1}{T}\sum_{t=1}^{T}\left|\bigvee_{i=1}^{k}F^{\alpha}(Z_{\boldsymbol{x}_i}^{(t)}) - \bigvee_{j=1}^{s}F^{\beta}(Z_{\boldsymbol{y}_j}^{(t)})\right|\right|$$

$$+\left|\frac{1}{2}\frac{1}{T}\sum_{t=1}^{T}\left|\bigvee_{i=1}^{k}F^{\alpha}(Z_{\boldsymbol{x}_i}^{(t)}) - \bigvee_{j=1}^{s}F^{\beta}(Z_{\boldsymbol{y}_j}^{(t)})\right| - \frac{1}{2}E\left|\bigvee_{i=1}^{k}F^{\alpha}(Z_{\boldsymbol{x}_i}^{(t)}) - \bigvee_{j=1}^{s}F^{\beta}(Z_{\boldsymbol{y}_j}^{(t)})\right|\right|.$$

The second term converges almost surely to zero by the strong Law of Large Numbers.

In what concerns the first term we have

$$\left|\frac{1}{2}\frac{1}{T}\sum_{t=1}^{T}\left|\bigvee_{i=1}^{k}\widehat{F}_{\boldsymbol{x}_i}^{\alpha}\left(Z_{\boldsymbol{x}_i}^{(t)}\right) - \bigvee_{j=1}^{s}\widehat{F}_{\boldsymbol{y}_j}^{\beta}(Z_{\boldsymbol{y}_j}^{(t)})\right| - \frac{1}{2}\frac{1}{T}\sum_{t=1}^{T}\left|\bigvee_{i=1}^{k}F^{\alpha}(Z_{\boldsymbol{x}_i}^{(t)}) - \bigvee_{j=1}^{s}F^{\beta}(Z_{\boldsymbol{y}_j}^{(t)})\right|\right|$$

$$\leq \frac{1}{2}\frac{1}{T}\sum_{t=1}^{T}\left|\left|\bigvee_{i=1}^{k}\widehat{F}_{\boldsymbol{x}_i}^{\alpha}\left(Z_{\boldsymbol{x}_i}^{(t)}\right) - \bigvee_{j=1}^{s}\widehat{F}_{\boldsymbol{y}_j}^{\beta}(Z_{\boldsymbol{y}_j}^{(t)})\right| - \left|\bigvee_{i=1}^{k}F^{\alpha}(Z_{\boldsymbol{x}_i}^{(t)}) - \bigvee_{j=1}^{s}F^{\beta}(Z_{\boldsymbol{y}_j}^{(t)})\right|\right|$$

$$\leq \frac{1}{2}\frac{1}{T}\sum_{t=1}^{T}\left|\bigvee_{i=1}^{k}\widehat{F}_{\boldsymbol{x}_i}^{\alpha}\left(Z_{\boldsymbol{x}_i}^{(t)}\right) - \bigvee_{j=1}^{s}\widehat{F}_{\boldsymbol{y}_j}^{\beta}(Z_{\boldsymbol{y}_j}^{(t)}) - \bigvee_{i=1}^{k}F^{\alpha}(Z_{\boldsymbol{x}_i}^{(t)}) + \bigvee_{j=1}^{s}F^{\beta}(Z_{\boldsymbol{y}_j}^{(t)})\right|$$

$$\leq \frac{1}{2}\frac{1}{T}\sum_{t=1}^{T}\left[\bigvee_{i=1}^{k}\left|\widehat{F}_{\boldsymbol{x}_i}^{\alpha}\left(Z_{\boldsymbol{x}_i}^{(t)}\right) - F^{\alpha}(Z_{\boldsymbol{x}_i}^{(t)})\right| + \bigvee_{j=1}^{s}\left|\widehat{F}_{\boldsymbol{y}_j}^{\beta}(Z_{\boldsymbol{y}_j}^{(t)}) - F^{\beta}(Z_{\boldsymbol{y}_j}^{(t)})\right|\right]$$

$$\leq \frac{1}{2}\frac{1}{T}\sum_{t=1}^{T}\left[\sum_{i=1}^{k}\left|\widehat{F}_{\boldsymbol{x}_i}^{\alpha}\left(Z_{\boldsymbol{x}_i}^{(t)}\right) - F^{\alpha}(Z_{\boldsymbol{x}_i}^{(t)})\right| + \sum_{j=1}^{s}\left|\widehat{F}_{\boldsymbol{y}_j}^{\beta}(Z_{\boldsymbol{y}_j}^{(t)}) - F^{\beta}(Z_{\boldsymbol{y}_j}^{(t)})\right|\right],$$

which converges almost surely to zero according to Gilat and Hill [8] (proof of Theorem 1.1). □

(Received February 7, 2013)

REFERENCES

[1] J. Beirlant, Y. Goegebeur, J. Segers, and J. Teugels: Statistics of Extremes: Theory and Applications. John Wiley 2004. DOI:10.1002/0470012382

[2] D. Cooley, P. Naveau, and P. Poncet: Variograms for spatial max-stable random fields. Dependence in Probability and Statistics *187* (2006), 373–390. DOI:10.1007/0-387-36062-x_17

[3] S. G. Coles: Regional modelling of extreme storms via max-stable processes. J. Roy. Statist. Soc. B *55* (1993), 797–816.

[4] L. de Haan: A spectral representation for max-stable proesses. Ann. Probab. *12* (1984), 1194–1204. DOI:10.1214/aop/1176993148

[5] L. de Haan and J. Pickands: Stationary min-stable stochastic processes. Probab. Theory Related Fields *72* (1986), 477–492. DOI:10.1007/bf00344716

[6] J. D. Fermanian, D. Radulovic, and M. Wegkamp: Weak convergence of empirical copula processes. Bernoulli *10* (2004), 847–860. DOI:10.3150/bj/1099579158

[7] H. Ferreira: Dependence between two multivariate extremes. Statist. Probab. Lett. *81* (2011), 5, 586–591. DOI:10.1016/j.spl.2011.01.014

[8] D. Gilat and T. Hill: One-sided refinements of the strong law of large numbers and the Glivenko–Cantelli Theorem. Ann. Probab. *20* (1992), 1213–1221. DOI:10.1214/aop/1176989688

[9] A. Krajina: An M-Estimator of Multivariate Dependence Concepts. Tilburg University Press, Tilburg 2010.

[10] P. Naveau, A. Guillou, D. Cooley, and J. Diebolt: Modelling pairwise dependence of maxima in space. Biometrika *96* (2009), 1, 1–17. DOI:10.1093/biomet/asp001

[11] G. Neuhaus: On the weak convergence of stochastic processes with multidimensional time parameter. Ann. Math. Statist. *42* (1971), 4, 1285–1295. DOI:10.1214/aoms/1177693241

[12] S. I. Resnick: Extreme Values, Regular Variation and Point Processes. Springer-Verlag, Berlin 1987. DOI:10.1007/978-0-387-75953-1

[13] M. Ribatet: A User's Guide to the Spatial Extremes Package. Unpublished, 2009. cran.r-project.org/web/packages/SpatialExtremes/vignettes/SpatialExtremesGuide.pdf

[14] M. Schlather: Models for stationary max-stable random fields. Extremes *5* (2002), 1, 33–44. DOI:10.1023/a:1020977924878

[15] M. Schlather and J. Tawn: A dependece measure for multivariate and spatial extreme values: Properties and inference. Biometrika *90* (2003), 139–156. DOI:10.1093/biomet/90.1.139

[16] R. L. Smith: Max-stable processes and spatial extremes. Unpublished manuscript, 1990. www.stat.unc.edu/postscript/rs/spatex.pdf

[17] R. L. Smith and I. Weissman: Characterization and Estimation of the Multivariate Extremal Index. Technical Report, Department of Statistics, University of North Carolina 1996. www.stat.unc.edu/postscript/rs/extremal.pdf

[18] A. Van Der Vaart and J. A. Wellner: Weak Convergence and Empirical Processes. Springer-Verlag, New York 1996. DOI:10.1007/978-1-4757-2545-2

[19] P. Vatan: Max-infinite divisibility and max-stability in infinite dimensions. Probability in Banach Spaces V, Lect. Notes in Math. *1153* (1985), 400–425. DOI:10.1007/bfb0074963

[20] Z. Zhang and R. L. Smith: The behavior of multivariate maxima of moving maxima processes. J. Appl. Probab. *41* (2004), 4, 1113–1123. DOI:10.1239/jap/1101840556

[21] Z. Zhang and R. L. Smith: On the estimation and application of max-stable processes. J. Statist. Planning Inference *140* (2010), 5, 1135–1153. DOI:10.1016/j.jspi.2009.10.014

Cecília Fonseca, Instituto Politécnico da Guarda. Portugal.
e-mail: cfonseca@ipg.pt

Luísa Pereira, Department of Mathematics, Universidade da Beira Interior, Covilhã, Portugal.
e-mail: lpereira@ubi.pt

Helena Ferreira, Department of Mathematics, Universidade da Beira Interior, Covilhã, Portugal.
e-mail: helenaf@ubi.pt

Ana Paula Martins, Department of Mathematics, Universidade da Beira Interior, Covilhã, Portugal.
e-mail: amartins@ubi.pt